

AN UNIFIED STATISTICAL PROCEDURE TO ANALYSE IRREVERSIBLE THERMAL CURVES

JHIMLI BHATTACHARYYA, GOPINATHA SURESH KUMAR, SOUVIK MAITI, DAISUKE MIYOSHI,
AND SANJAY CHAUDHURI

ABSTRACT. The phenomenon of hysteresis is commonly observed in many UV thermal experiments involving unmodified or modified nucleic acids. In presence of hysteresis the thermal curves are irreversible and demand a significant effort to produce the reaction specific kinetic and thermodynamic parameters. In this article we describe a unified statistical procedure to analyse such thermal curves. Our method applies to experiments with intramolecular as well as intermolecular reactions. More specifically, the proposed method allows one to handle the thermal curves for the formation of duplexes, triplexes and various quadruplexes in exactly the same way. The proposed method uses a local polynomial regression for finding the smoothed thermal curves and calculate their slopes. This method is more flexible and easy to implement than the least squares polynomial smoothing which is currently almost universally used for such purposes. Full analyses of the curves including computation of kinetic and thermodynamic parameters can be done using freely available statistical softwares. At the end, we illustrate our method by analysing irreversible curves encountered in the formations of a G-quadruplex and a LNA-modified parallel duplex.

1. INTRODUCTION

Analysis of experimental data is an integral part of chemical research. Even if a chemical experiment is well designed and extremely well executed, no conclusions can be drawn from it unless the results are properly analyzed. In fact, erroneous analysis of experimental data can lead to wrong conclusions, resulting in a huge waste of effort and resources.

Data obtained from chemical experiments require several advanced statistical tools for a proper analysis. Each of these steps are computationally intensive and demands an advanced mathematical and statistical expertise from a researcher. Many procedures require tedious calculations, too difficult and time consuming to perform without advanced computational facilities. Many researchers use computational tools designed specifically for their own needs.(Nakano et al., 2004; Miyoshi et al., 2006, 2009; Ray et al., 1996; Mirzoev and Lyubartsev, 2013) However, in most cases no statistical software is freely available. Many commercial softwares focus only on a part of the task and different softwares are required to complete the procedure. Lack of analytic tools often restrict choices at the design stage of the experiment and more often inflates the cost and effort even with a loss of accuracy.

As an example, we can cite the thermodynamic and kinetic analyses of hybridization reactions involving various unmodified and modified nucleic acids which have been a topic of immense interest among the researchers in biophysical chemistry for at least half a century. Such investigations can be helpful in determining the stability of the secondary structures in nucleic acids. They can also be used to study the hybridization between an oligonucleotide and a specific target. Results from these studies are useful for PCR primer design, gene sequencing and a host of bio-medical applications. In order to study the biophysical characteristics of any nucleic acid hybridization reaction spectrophotometrically, UV thermal experiments are useful. For nucleic acids, denaturation (heating/melting) and renaturation (cooling/annealing) processes are usually reversible. (Mergny and Lacroix, 2003) That is, if a sample of denatured nucleic acid is cooled, in most cases renaturation of the structure is observed. Thermodynamic parameters can be obtained by analyzing such thermal curves, (Nakano et al., 2004; Miyoshi et al., 2006, 2009; Mergny and Lacroix, 2003; Sugimoto et al., 2001; Rougée et al., 1992) provided the denaturation (melting) and renaturation (annealing) curves can be superimposed on each other (*i.e* the folding and unfolding rate constants of the nucleic acids are equal). With many modified and unmodified oligonucleotides however, such is not the case. For various reasons the renaturation process may be quite slow.(Mergny and Lacroix, 2003; Cantor and Schimmel, 1980; Brown et al., 2005) As a result, if the temperature gradient during the melting and annealing is not slow

enough, the heating and cooling curves are not superimposed and thus none of them correspond to the true equilibrium curve. (Mergny and Lacroix, 2003) This phenomenon is known as hysteresis.

Hysteresis has been discussed by several authors before. Anshelevich et al. (1984) perform a theoretical study of melting processes where hysteresis is observed. A classic example can be seen during the fast melting and annealing of calf thymus DNA. (Cantor and Schimmel, 1980) In recent times, such a phenomenon has been reported from the study of RNA and DNA binding to a pyrrolidine-amide oligonucleotide mimic (POM) (Hickman et al., 2000) and the hybridization of locked nucleic acid (LNA) modified non canonical structures. (Kaur et al., 2007; Bhattacharyya et al., 2011) Rougée et al. (1992) reported and analyzed non-equilibrium thermal curves in triplex formation. It has also been observed in triplex formation of DNA oligomers with Guanidinium and methylthiourea-link nucleosides. (Blaskó et al., 1996; Arya and Bruce, 1999) Same phenomenon was seen in triplex formation with α -L-LNA (Kumar et al., 2006) and peptide nucleic acids (PNA). (Lesnik et al., 1997) It is known that melting of tetramolecular DNA and RNA quadruplexes is not kinetically reversible. (Mergny et al., 2005; Tran et al., 2013) However, for other, specially the intramolecular G-quadruplexes hysteresis is commonly observed. (Mergny and Lacroix, 2001, 2003; Brown et al., 2005; Saccà et al., 2005; Zhang and Balasubramanian, 2012; Pandey et al., 2013)

If hysteresis is observed, the thermodynamic parameters cannot be estimated directly from the thermal curves. Nevertheless, it is possible to observe a simple one way reaction from a folded state to an unfolded state with a melting curve, whereas the annealing curve traces the transition from an unfolded random coil to a folded hybrid. Thus, if hysteresis is observed, kinetic analysis of melting and annealing curves can be attempted. (Bhattacharyya et al., 2011) The annealing and melting curves respectively allow one to determine the association and dissociation rate constants. Assuming a two state (all or none) model, these kinetic rate constants yield the corresponding activation energies. From these rate constants and the activation energies, thermodynamic parameters, *e.g.* changes in free energy, enthalpy or entropy can be obtained. The analysis mentioned above was first described by Rougée et al. (1992) and has been successfully used for kinetic analysis of many non-canonical structures. However, as we shall demonstrate below, it is pretty laborious to perform this kinetic analysis manually. First of all, the raw experimental data has to be smoothed and the value of the derivative has to be accurately calculated at each observation. The values of rate constants at each temperature are obtained by solving a pair of simultaneous equations. The activation energies are calculated from the rates of changes in the two rate constants. To our knowledge, no software which tackles the whole procedure is available. In most cases if the UV thermal curves show hysteresis, estimation of the kinetic parameters, activation energies and hence the thermodynamic profile become extremely time consuming. Thus in such cases thermodynamic analysis is often not attempted from the spectrophotometric data. However, a thorough thermodynamic profile is necessary to understand the chemical interactions of nucleic acids. This thermodynamic profile complements the structural data providing a clear and coherent picture. (Kaur et al., 2007, 2008; Sugimoto et al., 2001; Das et al., 2011; Bhadra and Suresh Kumar, 2011; Saha et al., 2010)

In this article we describe a unified statistical procedure for kinetic analysis of UV thermal curves showing hysteresis. Our procedure can be implemented using freely available libraries and codes from a statistical software called R. (R Core Team, 2012) We use local polynomial regression method to smooth the raw experimental data and estimate the derivative of the underlying thermal curve at each temperature. Our software calculates the kinetic rate constants, activation energies and the thermodynamic parameters using R as well. We illustrate our procedure with two data from four sets of thermal curves. The first two sets consider intramolecular G-quadruplex formation of two specific RNA strands. Stability of these nucleic acids were investigated by Pandey et al. (2013), who however, in order to avoid hysteresis performed the experiment with a flatter temperature gradient than the data used here. Next, we use data reported by Bhattacharyya et al. (2011) where kinetic and thermodynamic effects of LNA modification on parallel and antiparallel DNA duplexes were reported. Significant hysteresis was observed for LNA modified parallel duplexes for all temperature gradients used. The extent of hysteresis increased with the increase in the number LNA modifications. Our results closely match with those reported in the original references.

2. UV SPECTROPHOTOMETRIC EXPERIMENT TO OBTAIN THE THERMAL CURVES

The UV absorbance spectra are recorded on a spectrophotometer equipped with a temperature controller. The heating and cooling rates are usually kept constant throughout the experiment. The sample is usually

first annealed from a high (95° C) to a low (0° C) temperature at a steady rate. The annealed sample is then incubated at the low temperature for some time. When the temperature is below 20°C the cell chamber is flushed with dry nitrogen gas to avoid condensation. Then at the melting stage the temperature is steadily increased from low to a high value. The annealing and the melting curves are usually obtained by measuring the UV absorbance at 260 or 295 nm. A buffer is used to control the pH of the system. The final data is obtained by subtracting the absorbance due to the buffer from the observed data.

3. THE THEORY BEHIND THE KINETIC AND THERMODYNAMIC ANALYSIS OF THERMAL CURVES EXHIBITING HYSTERESIS

In presence of hysteresis, for a kinetic analysis of the thermal curves one uses a two-state model between the reactant (R) and the product (P). Many situations are possible in this case. For example, a single strand can fold into a duplex or a more complex hybrid. The reaction may be bimolecular involving either two autocomplimentary oligoes or two different complimentary oligonucleotides. The kinetic order of the reaction differs from one group to another. We consider two broad classes of reactions discussed in Table 2 of Mergny and Lacroix (2003) below. Pronounced hysteresis have been observed by several authors, for reactions belonging to these classes.

3.0.1. *Intramolecular reactions.* For intramolecular reactions, a monomeric nucleic acid strand (R) folds to produce various hybrid structures (P). Hairpin duplex, intramolecular triplex, intramolecular G-quadruplex formations are examples belonging to this class.

At equilibrium, the reaction can be written as:



Suppose k_{on} denotes the rate constant of annealing or cooling, which means association and k_{off} is the rate constant of melting or heating which results in dissociation. From (1) the rate of change of concentration of the product P at time t is given by

$$(2) \quad \frac{d[P]}{dt} = k_{\text{on}}[R] - k_{\text{off}}[P].$$

Notice that, (1) is a first order reaction. The equilibrium would be independent of the initial concentration of the reactant.

3.0.2. *Intermolecular reactions with two complimentary oligoes.* For this class of reactions two complimentary oligoes R_1 and R_2 hybridize to form the product P . This class of reactions is large and includes most of the hybridization reactions involving various nucleic acids. Hysteresis is quite commonly observed in this group of reactions. As for example, R_1 and R_2 may both be single stranded oligoes which hybridize to produce a duplex. Bhattacharyya et al. (2011) observed hysteresis in parallel duplex formation where one of the constituent strand was modified by LNA. Similar examples of hysteresis in duplex formation abound.(Hickman et al., 2000; Kaur et al., 2007) Various triplex formations where one of the reactants is a duplex and the other a single strand also show pronounced hysteresis. (Rougée et al., 1992; Arya and Bruice, 1999; Kumar et al., 2006)

The reaction in this case is of second order. At equilibrium it can be expressed as:(Mergny and Lacroix, 2003; Kaur et al., 2007; Bhattacharyya et al., 2011)



As before, if we assume k_{on} and k_{off} respectively denote the rate constants of annealing and melting, from (3) the rate of change of concentration of the product P at time t is given by

$$(4) \quad \frac{d[P]}{dt} = k_{\text{on}}[R_1][R_2] - k_{\text{off}}[P].$$

It is clearly seen that unlike the intramolecular reactions, the equilibrium in a bimolecular reaction depends on the initial concentration of the two reactants.

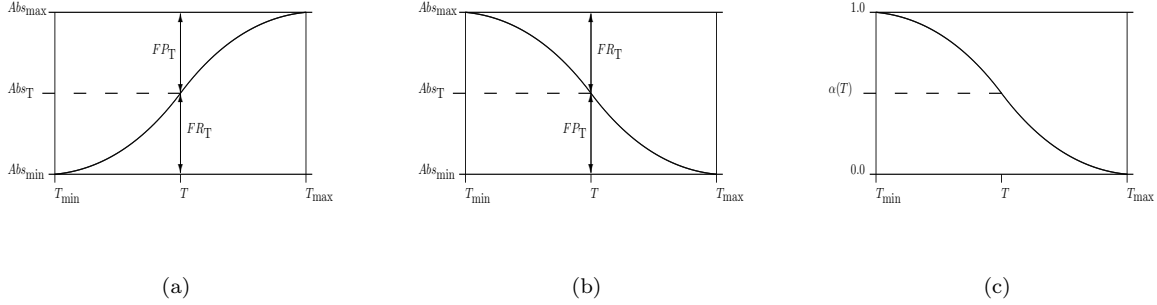


FIGURE 1. A schematic curve of absorbance at 260 nm 1(a) and at 295 nm 1(b). Hyperchromicity is observed in the former and not in the latter. FR_T and FP_T are respectively the fraction of reactant and the product at temperature T . Notice that, depending on the presence and absence of hyperchromicity, the definitions of FR_T and FP_T change in the plot. 1(c) A schematic diagram of $FP_T = \alpha(T)$ obtained from equations (7) and (8) below.

3.0.3. *Kinetic and Thermodynamic equations in presence of hysteresis.* In both (2) and (4) the temperature is held fixed. The concentration would vary with time, rate constants k_{on} , k_{off} would remain fixed. If the temperature T increase or decrease with time as well, the concentration as well as the rate constants will vary with it. If dT/dt denotes the rate of change of T at time t , (2) and (4) can respectively be re-expressed as

$$(5) \quad \frac{d[P]}{dT} = \left(\frac{dT}{dt} \right)^{-1} \left\{ k_{on}[R] - k_{off}[P] \right\}$$

and

$$(6) \quad \frac{d[P]}{dT} = \left(\frac{dT}{dt} \right)^{-1} \left\{ k_{on}[R_1][R_2] - k_{off}[P] \right\}.$$

Here k_{on} , k_{off} and the concentrations are taken to vary with T .

We assume that the fraction of the product P , at temperature T , denoted by $\alpha(T)$ can be obtained from the absorbance of the heating and cooling curves at temperature T . Suppose $Abs(T)$ is the absorbance at temperature T , Abs_{min} and Abs_{max} are respectively the minimum and maximum absorbance of the thermal curve under consideration. The formula to obtain $\alpha(T)$ is determined by the presence or absence of hyperchromicity at the wavelength being used in the experiment. If hyperchromicity is observed, *e.g.* duplex formation observed at 260 nm, the absorbance increases with temperature. That is higher absorbance implies higher fraction of single strands (see Figure 1(a) above). In such cases the fraction of product at any temperature T is calculated: (Kumar et al., 2006; Kaur et al., 2007; Bhattacharyya et al., 2011)

$$(7) \quad \alpha(T) = \frac{Abs_{max} - Abs(T)}{Abs_{max} - Abs_{min}}.$$

On the other hand in the absence of hyperchromicity, *e.g.* triplex formation reaction recorded at 295 nm, (Mergny and Lacroix, 2003) absorbance decreases with the increase in fraction of the single strands (see Figure 1(b)). Thus the fraction of triplex should be calculated using the formula: (Arora and Maiti, 2009)

$$(8) \quad \alpha(T) = \frac{Abs(T) - Abs_{min}}{Abs_{max} - Abs_{min}}.$$

Note that, by our definition for both (7) and (8), $0 \leq \alpha(T) \leq 1$, $\alpha(T_{min}) = 1$ which is the completely hybridized state and $\alpha(T_{max}) = 0$ which corresponds to the completely dissociated state. A schematic plot of $\alpha(T)$ with temperature for both cases is shown in Figure 1(c) above. Since the fraction decreases with

temperature, the derivative is negative. This implies that the *Van't Hoff* temperatures *i.e.* the apparent temperatures of mid-transition in the melting and annealing phases can be approximated by the temperature corresponding to minimum value of this derivative.

Our choice of the Abs_{max} and Abs_{min} as baselines, constant over the values of T is a special case in a set of possible choices of baselines. Many researchers, specially Mergny and his co-authors suggest that time dependent baselines are more appropriate and strongly recommend their use throughout. (Mergny and Lacroix, 2001, 2003, 2009) The kinetic and thermodynamic parameters computed from the experimental data would change if the baselines are changed. In that sense, the choice of baselines are crucial. However, there is no objective way of finding them. In most cases, baselines that are linear with temperature are used. Even then, the choice of their slopes and intercepts are subjective. In some cases (eg. Rougée et al. (1992)) baselines were obtained through separate experiments. For intramolecular G-quadruplex formation without any evidence of hysteresis, such baselines have been obtained through model fitting. (Arora and Maiti, 2009) Many authors however, prefer constant baselines. (Arya and Bruice, 1999; Blaskó et al., 1996; Kumar et al., 2006; Bhattacharyya et al., 2011) Our choice is in line with them.

We should also note that, in equations (7) and (8) we have made an implicit assumption that a melting curve always begin with a fully (*i.e.* 100%) folded state and end at a fully unfolded state, where as an annealing curve start and end respectively with a fully denatured and renatured states. This may not hold in many cases. As for example, if the temperature of midtransition is too low (eg. 20° C or below), structure of the corresponding DNA may be too unstable to fold perfectly at 0° C. As a result the melting curve will not start from a 100% denatured state. On the other hand, in presence of K^+ ions G-Quadruplexes are too stable and a melting curve involving such DNA structures may not end at a fully denatured state. However, equations (7) and (8) are still relevant. If there is evidence that the nucleic acid is not fully folded at 0° C or fully unfolded at 95° C, the observed thermal curves are extrapolated beyond this range to determine the temperatures corresponding to fully renatured and denatured states. We don't discuss the actual procedure for such extrapolation here, but equations (7) and (8) can be applied to the extrapolated curves as well.

In presence of hysteresis, the concentration of the product at any temperature T is different on the annealing and melting curves. Let $\alpha_h^{(1)}(T)$ and $\alpha_c^{(1)}(T)$ respectively denote the association and dissociation rates of the product at temperature T . From equations (5) and (6), assuming equal stoichiometric ratios of the reactants in (6) and $(|dT/dt|)^{-1} = \gamma$, we get:

$$(9a) \quad \alpha_h^{(1)}(T) = \frac{d\alpha_h}{dT} = \gamma [k_{on}(1 - \alpha_h) - k_{off}\alpha_h],$$

$$(9b) \quad \alpha_c^{(1)}(T) = \frac{d\alpha_c}{dT} = -\gamma [k_{on}(1 - \alpha_c) - k_{off}\alpha_c].$$

and

$$(10a) \quad \alpha_h^{(1)}(T) = \frac{d\alpha_h}{dT} = \gamma [k_{on}C(1 - \alpha_h)^2 - k_{off}\alpha_h],$$

$$(10b) \quad \alpha_c^{(1)}(T) = \frac{d\alpha_c}{dT} = -\gamma [k_{on}C(1 - \alpha_c)^2 - k_{off}\alpha_c].$$

Here C is the molar concentration of the reactant strands in (6). Notice that, in (10b), T decreases with time, so $(dT/dt)^{-1} = -\gamma$.

Equations (9a) and (9b) do not depend on the initial concentration of the reactant strand. This again indicates that the equilibrium is not dependent on the concentration factor in this case. The assumption that the concentrations of two reactant strands are equal is crucial for equations (10a) and (10b). In the general case these equations would be a bit more complex. (Rougée et al., 1992; Blaskó et al., 1996)

For any experiment C and γ are specified by the design. Thus in order to calculate the rate constants k_{on} and k_{off} at a given temperature T , one needs to find out α_h , α_c , $d\alpha_h/dT$ and $d\alpha_c/dT$ at temperature T and solve the equations (10a) and (10b).

Once the values of k_{on} and k_{off} are known for each temperature T , the thermodynamic parameters can be obtained from these values using the *Arrhenius equation*. The change in the Free Energy at the temperature T (*i.e.* ΔG_T°) can be directly obtained as $-RT \log(k_{on}/k_{off})$, where k_{on} and k_{off} are the values of the rate constants at temperature T .

The activation energies of annealing (E_{on}) and melting (E_{off}) are related to k_{on} and k_{off} through the Arrhenius equations,

$$(11) \quad \log(k_{\text{on}}) = \log(A_{\text{on}}) - \frac{E_{\text{on}}}{RT},$$

$$(12) \quad \log(k_{\text{off}}) = \log(A_{\text{off}}) - \frac{E_{\text{off}}}{RT}.$$

The other two thermodynamic parameters, *i.e.* the change in enthalpy, $\Delta H^\circ = E_{\text{on}} - E_{\text{off}}$ and the product of temperature and the change in entropy $T\Delta S^\circ = \Delta H^\circ - \Delta G_T^\circ$ can be computed once E_{on} and E_{off} is known.

Values of the pairs $(A_{\text{on}}, E_{\text{on}})$ and $(A_{\text{off}}, E_{\text{off}})$ can be determined from the *Arrhenius plot* of $\log(Ck_{\text{on}})$ vs. $1/T$ and $\log(k_{\text{off}})$ vs. $1/T$ respectively. In particular, E_{on} and E_{off} are obtained from the slopes of the plots. We discuss this topic in more details in Section 4.0.3 below.

In equations (9) and (10), we have assumed that the absolute values of both the rates of cooling and heating respectively at the annealing and melting phases are γ . That is, the rate at which the temperature goes down at the cooling phase and the rate at which it goes up at the heating phase are equal. Simple calculations show that in such cases, the slopes of the Arrhenius plots do not depend on γ . This proves that the change in enthalpy, ΔH° does not depend on γ either. Furthermore, even though the intercepts of the Arrhenius plots depend on γ , it can be shown that the ratio of the kinetic rate constants *i.e.* $k_{\text{on}}/k_{\text{off}}$ is still independent of it. As a result ΔG_T° and $T\Delta S^\circ$ are independent of γ as well. This implies that even if for some reason γ is specified wrong, the kinetic analyses as described above would produce correct values of the thermodynamic parameters.

We conclude this section by noting that T_m , *i.e.* the temperatures of mid-transition for the intramolecular and intermolecular reactions considered satisfy $\Delta G_{T_m} = 0$ and $\Delta G_{T_m} = RT_m \log(C/2)$ respectively. (Mergny and Lacroix, 2003) Later we show how T_m can be estimated from the non-equilibrium thermal curves using our procedure.

4. A STATISTICAL PROCEDURE FOR DATA ANALYSIS

Suppose $\alpha_{ci} = \alpha_c(T_i)$ and $\alpha_{hi} = \alpha_h(T_i)$, $i = 1, 2, \dots, n$ were observed at temperatures T_i , with $T_{i+1} - T_i$ constant for all i . In order to calculate the kinetic rate constants k_{on} and k_{off} using equations (10a) and (10b) one requires accurate values of absorbance and their rates of changes with the temperature from this experimental data. Clearly, $\alpha_{ci}^{(1)} = \alpha_c(T_i)/dT$ and $\alpha_{hi}^{(1)} = d\alpha_h(T_i)/dT$ cannot be recorded during the run of the experiment for any T_i . They have to be estimated from the recorded α_{ci} and α_{hi} values.

At any T_i , the fraction of the duplex $\alpha_i = \alpha(T_i)$ (for both the melting and annealing stages) is recorded with noise. Presence of this random noise makes the estimation of $\alpha_i^{(1)} = d\alpha(T_i)/dT$ difficult. It is well known that the first order difference quotients *i.e.* $r_i = (\alpha_{i+1} - \alpha_{i-1}) / (T_{i+1} - T_{i-1})$ can lead to extremely noisy and wrong estimates of $\alpha_i^{(1)}$. One possible solution used by several authors (eg. Kaur et al. (2007)) is first to smooth α_i and then use the first order difference quotients of the smoothed data to estimate the derivative.

Several methods of smoothing experimental data and estimating derivatives up to several orders have been discussed in Literature before. The most popular is the so called *Least-squares polynomial smoothing* (LSP) introduced by Savitzky and Golay (1964). Assuming equi-spaced data, for the smoothed value at α_i this method fits polynomials of degree up to five up to twenty five points around T_i . The article provides values of the coefficients for these smoothing polynomials and for the first to fifth derivatives. This method has been widely used computational chemistry. The five-point third degree LSP is used in many standard data-acquisition hardware and software packages.

In an article Marchand and Marmet (1983) discuss several pitfalls of LSP method and propose a binomial smoothing filter as an alternative. Several other methods based on *smoothing splines*, *wavelets* etc. have been proposed. Wavelets are usually computationally demanding and the smoothing splines require one to make a crucial choice of the smoothing parameter. (Brabanter et al., 2013) In a recent article Brabanter

et al. (2013) discuss a new method to estimate $\alpha_i^{(1)}$ as a weighted sum of difference quotients of various orders from the un-smoothed data.

An alternative to all these methods are provided by *local polynomial regression* (LPR). This method provides an computationally efficient and easily implementable way to smooth the noisy data and estimate its derivatives.

4.0.1. *Local Polynomial Regression.* In local polynomial regression (LPR), one estimates the smoothed curve and its derivatives by fitting a polynomial within a local neighborhood of each point.

The data is assumed to be generated from the model

$$(13) \quad \alpha = m(T) + \epsilon,$$

for some unknown function m of temperature T . The variable ϵ is the random noise, with $E[\epsilon] = 0$ and $Var[\epsilon] = \sigma^2$. If we assume that the $(p + 1)$ th derivative of m exist, we can locally approximate m by a polynomial of order p . For any point T_0 strictly with in the range of the temperature concerned and for any T in a neighborhood of T_0 , a Taylor series expansion yields, (Wand and Jones, 1995; Brabanter et al., 2013)

$$(14) \quad m(T) \approx m(T_0) + m^{(1)}(T_0)(T - T_0) + \dots + \frac{m^{(j)}(T_0)}{j!}(T - T_0)^j + \dots + \frac{m^{(p)}(T_0)}{p!}(T - T_0)^p.$$

Here $m^{(j)}(T_0)$ is the value of the j th derivative of m at T_0 . Note that, none of the derivatives are known and has to be estimated from the data.

Equation (14) can be re written as:

$$(15) \quad m(T) \approx \sum_{j=0}^p \frac{m^{(j)}(T_0)}{j!} (T - T_0)^j = \sum_{j=0}^p \beta_j (T - T_0)^j.$$

An estimate of the unknown vector of coefficients $\beta = (\beta_0, \beta_1, \dots, \beta_p)$ in (15) denoted $\hat{\beta}$ is obtained as the solution to the weighted local least squares regression problem given by,

$$(16) \quad \hat{\beta} = \arg \min_{\beta} \sum_{i=1}^n \left\{ \alpha_i - \sum_{j=0}^p \beta_j (T_i - T_0)^j \right\}^2 \frac{1}{h} K \left(\frac{T_i - T_0}{h} \right).$$

We note that, the expression in (14) and (15) are local. Thus $\hat{\beta}$ will be different for different T_0 .

The *kernel* function K and the pre-specified bandwidth h in (16) controls the weights put on the individual observations as well as the size of the neighborhood of T_0 used in estimating $m(T_0)$. The kernel function K has to satisfy certain properties, which we don't discuss in this article (see Wand and Jones (1995) for details). There are several choices for K . Some popular ones are,

$$(17) \quad K(x) = \frac{1}{2} 1_{\{|x| < 1\}}, \quad (\text{Uniform})$$

$$(18) \quad K(x) = \frac{3}{4} (1 - x^2) 1_{\{|x| < 1\}}, \quad (\text{Epanechnikov})$$

$$(19) \quad K(x) = (2\pi)^{-1/2} e^{-x^2/2}. \quad (\text{Gaussian})$$

Each Kernel puts more weight on the observations nearer to T_0 than those which are further away. It may put zero weight on some observations, as in (17) and (18) above. The Gaussian kernel (19) is positive for all values of x and thus takes into account all observations, but the weights of observations further away than -3 and 3 are negligible.

The bandwidth h plays a crucial role. Small h would produce a non-smooth m essentially interpolating the data. A larger than necessary h would result in over-smoothing. For $p = 1$, when a straight line fitted locally, an optimal value of h can be obtained from the observed data. We refer to Wand and Jones (1995) for details.

Once the kernel K and bandwidth h is specified, at any T_0 , $\hat{\beta}$ in (16) can be easily obtained using weighted regression. In fact, an analytic formula, involving only matrix manipulation to find $\hat{\beta}$ is available. From (15) the estimate of $m(T_0)$ and $\alpha(T_0)$, denoted $\hat{\alpha}(T_0) = \hat{m}(T_0) = \hat{\beta}_0$.

4.0.2. *Derivative Estimation.* Using LPR technique, any point T_0 the value of $m^{(j)}(T_0)$ can be easily estimated. From (15), the estimate is simply given by:

$$(20) \quad \widehat{m^{(j)}}(T_0) = j! \cdot \hat{\beta}_j.$$

Thus the estimated value of $\alpha^{(1)}(T_0)$ (denoted $\hat{\alpha}^{(1)}(T_0)$) is simply $\hat{\beta}_1$ obtained from LPR at T_0 .

The estimate in (20) is in general different from the derivative of \hat{m} at T_0 . In fact, the latter would be a bad estimate for noisy data especially for large values of j . (Brabanter et al., 2013)

The accuracy of $\widehat{m^{(j)}}$ depends on the value of p i.e the order of the polynomial being fit locally. It can be shown that (Wand and Jones, 1995) in order to estimate the j th derivative, a in some sense it is better to choose p such that $p - j$ is an odd number.

We close this section by making two comments. First of all, for LPR it is not strictly required that the temperatures T_i be equi-spaced. Furthermore, T_0 does not need to equal T_i for any i . It is sufficient that T_0 is a point within the range of observed temperatures. Thus we can estimate α and $\alpha^{(1)}$ on a temperature grid finer than width γ . It is not also required to use that same bandwidth for the whole data. It is natural often to use different bandwidth for different T_0 . Several adaptive procedures to obtain such optimal variable local bandwidths are available. However, LPR would not be give accurate results T_0 is too close to the boundary. This is an inconvenience common to many smoothing techniques.

4.0.3. *Kinetic and Thermodynamic Parameter Estimation.* The smoothed values of α_{ci} (i.e $\hat{\alpha}_{ci}$), $\alpha_{ci}^{(1)}$ (i.e $\hat{\alpha}_{ci}^{(1)}$) and those of α_{hi} (i.e $\hat{\alpha}_{hi}$), $\alpha_{hi}^{(1)}$ (i.e $\hat{\alpha}_{hi}^{(1)}$) can be determined using LPR for all values of T_i from the annealing and melting curves respectively. Once these values are available, depending on the system, equations (9a),(9b) or (10a),(10b) can be solved at each T_i to obtain the values of Ck_{on} and k_{off} at T_i . Here for convenience we take $C = 1$ for intramolecular reactions.

If hysteresis is observed, the apparent half temperatures of the annealing and melting phase denoted $T_{1/2\text{-anneal}}$ and $T_{1/2\text{-melt}}$ respectively will be far apart. They are the temperatures at which the minimum values of $\hat{\alpha}_c^{(1)}$ and $\hat{\alpha}_h^{(1)}$ were respectively obtained.

In order to estimate the activation energies E_{on} and E_{off} the Arrhenius Plot is used. Because of larger change in the absorbance on the annealing and melting curves around respective $T_{1/2\text{-anneal}}$ and $T_{1/2\text{-melt}}$ k_{on} and k_{off} can be accurately measured around these temperatures. Thus the Arrhenius Plot is drawn near these two temperatures.

In order to estimate A_{on} and E_{on} we perform a linear regression of $\log(Ck_{\text{on}})$ on $1/T$ around $T_{1/2\text{-anneal}}$. Suppose a_{on} and b_{on} are respectively the estimated intercept and slope of this fit. From (11) it is clear that the estimates of A_{on} (denoted \hat{A}_{on}) and E_{on} (denoted \hat{E}_{on}) are given by, $\log(\hat{A}_{\text{on}}) = a_{\text{on}} - \log(C)$ and $\hat{E}_{\text{on}} = -R \cdot b_{\text{on}}$.

Similarly, suppose a_{off} and b_{off} are respectively the estimated intercept and slope of the regression of $\log(k_{\text{off}})$ with $1/T$ around $T_{1/2\text{-melt}}$. Thus, from (12) one can find $\log(\hat{A}_{\text{off}}) = a_{\text{off}}$ and $\hat{E}_{\text{off}} = -R \cdot b_{\text{off}}$.

We can express the change in enthalpy in terms of b_{on} and b_{off} as

$$(21) \quad \Delta H^\circ = \hat{E}_{\text{on}} - \hat{E}_{\text{off}} = -R(b_{\text{on}} - b_{\text{off}}).$$

The change in free energy at any given temperature T^* is given by $\Delta G_{T^*}^\circ = -RT^* \log(k_{\text{on}}(T^*)) + RT^* \log(k_{\text{off}}(T^*))$. However, since the relation between k_{on} and k_{off} with T can only be accurately determined closer to $T_{1/2\text{-anneal}}$ and $T_{1/2\text{-melt}}$, Bhattacharyya et al. (2011) suggest using the predicted values obtained from the linear fits described above. Thus at T^* we get,

$$(22) \quad \log(k_{\text{on}}(T^*)) = a_{\text{on}} - \log(C) + \frac{b_{\text{on}}}{T^*},$$

$$(23) \quad \log(k_{\text{off}}(T^*)) = a_{\text{off}} + \frac{b_{\text{off}}}{T^*},$$

$$(24) \quad \Delta G_{T^*}^\circ = -RT^* \left\{ (a_{\text{on}} - \log(C) - a_{\text{off}}) + \frac{1}{T^*} (b_{\text{on}} - b_{\text{off}}) \right\}.$$

From the expressions of ΔH° and $\Delta G_{T^*}^\circ$ above, we can express $T^*\Delta S^\circ = \Delta H^\circ - \Delta G_{T^*}^\circ$ in terms of a_{on} , a_{off} , b_{on} and b_{off} . The explicit expression turns out to be,

$$(25) \quad T^*\Delta S^\circ = RT^*(a_{\text{on}} - \log(C) - a_{\text{off}}).$$

Clearly, ΔH° and $T^*\Delta S^\circ$ can be obtained directly from the linear fits on the Arrhenius plot. $\Delta G_{T^*}^\circ$ can then be calculated from ΔH° and $T^*\Delta S^\circ$.

4.0.4. *Finding the temperature of mid-transition.* The temperature of mid-transition T_m can be computed by solving (24) with known values of ΔG_{T_m} . For intramolecular reactions it is known that $\Delta G_{T_m} = 0$, which implies

$$(26) \quad T_m = \frac{b_{\text{off}} - b_{\text{on}}}{a_{\text{on}} - a_{\text{off}}} \text{ }^\circ\text{K}.$$

For intermolecular reactions with two complimentary oligoes $\Delta G_{T_m} = RT_m \log(C/2)$. This leads to

$$(27) \quad T_m = \frac{b_{\text{off}} - b_{\text{on}}}{a_{\text{on}} - a_{\text{off}} - \log(2)} \text{ }^\circ\text{K}.$$

In both cases T_m does not depend on either γ or C .

5. SOFTWARE IMPLEMENTATION

The whole procedure described in Section 4 can be implemented with available statistical softwares. For our purpose we use packages from a statistical repository called **R**. (R Core Team, 2012) This repository is completely free and contains the most up to date tools available to statisticians. Furthermore, one can easily write codes in **R** and thus all parts of the procedures mentioned above can be integrated in a single piece of code.

As we have mentioned before, determination of the bandwidth h used in LPR is crucial. A bad choice of h may produce a over or under smoothed solution, which will affect the values of k_{on} , k_{off} and other parameters at a later stage. We are not required to use the same h for all the points. The thermal curves do not change much near the two ends, but large changes in absorbance are observed around $T_{1/2\text{-anneal}}$ and $T_{1/2\text{-melt}}$. Thus it is advisable to use different bandwidths for different parts of the curves.

The optimal bandwidth depends on the choice of kernel function K as well. There is a vast literature in statistics dealing with determination of optimal global or local optimal bandwidths. We skip the technical details here.

For our purposes we use the a function named **lokerns** from the package named **lokern** (Herrmann and Maechler, 2013) in **R**. In order to find the smoothed values $\hat{\alpha}_{ci}$ of α_{ci} at any temperature T_i , the **lokerns** function uses Gaussian kernel to compute an adaptive local plug-in bandwidth. With this variable local bandwidth and using Gaussian kernel the values of $\hat{\alpha}_{ci}$ are finally calculated. The smoothed values $\hat{\alpha}_{hi}$ and derivatives $\hat{\alpha}_{ci}^{(1)}$ and $\hat{\alpha}_{hi}^{(1)}$ at each T_i are calculated similarly. We use separate runs of **lokerns** to calculate the above four functions. Thus the optimal local bandwidths for each of them are different. After obtaining $\hat{\alpha}_c^{(1)}$ and $\hat{\alpha}_h^{(1)}$, The values of $T_{1/2\text{-anneal}}$ and $T_{1/2\text{-melt}}$ can be easily obtained. One however, needs to be careful about the spurious low values of the derivatives near the ends of the temperature range.

From the available values of $\hat{\alpha}_{ci}$, $\hat{\alpha}_{hi}$, $\hat{\alpha}_{ci}^{(1)}$ and $\hat{\alpha}_{hi}^{(1)}$ at each T_i , it is easy to solve equations (10a) and (10b) to obtain the values of Ck_{on} and k_{off} . For the purpose of the Arrhenius plot it is sufficient to obtain these values near $T_{1/2\text{-anneal}}$ and $T_{1/2\text{-melt}}$. However, we compute Ck_{on} and k_{off} for all available temperatures. This is computationally wasteful but only slightly.

The linear fits in the Arrhenius plots are easily obtained using the **lm** function in **R**. From **lm** the values of a_{on} , b_{on} , a_{off} and b_{off} are obtained. The thermodynamic parameters at a temperature T^* are calculated from these using the formula in equations (21), (24) and (25).

6. ILLUSTRATIVE EXAMPLES

In this section we present two illustrative examples of the procedure described above. Our first example considers intramolecular G-Quadruplex formation of two specific RNA strands. In the second example we consider duplex formation by LNA modified DNA strands at two different pH values.

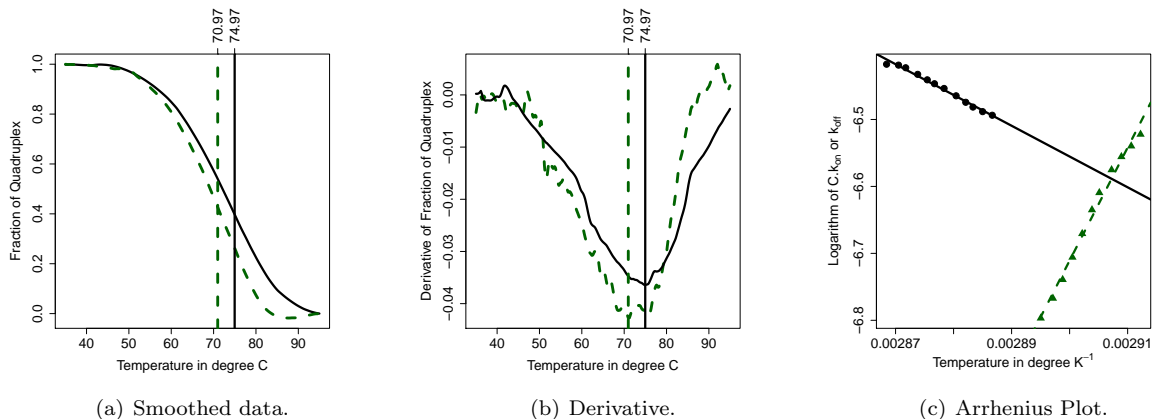


FIGURE 2. Smoothed curve 2(a), Derivative 2(b) and Arrhenius Plot 2(c) for the intramolecular G-quadruplex formation described in Pandey et al. (2013). The fraction of the Quadruplex was calculated using Equation (7). The results were obtained from the proposed software. The solid lines correspond to melting and the dashed lines correspond to annealing.

6.0.1. *Intramolecular G-Quadruplex formation.* Pandey et al. (2013) considered the effect of loops and G-quartets on the stability of RNA G-quadruplexes. We select two RNA strands from this article. They are namely, BAP1 (5'-GGGUGGGCCCUGGGC UCUGGG-3') and CCDC64 (5'-GGGCCCAUGGGUCCGGGAGGG-3'). For both of these strands hysteresis was observed for a temperature gradient of 0.25°C per minute.

The fitted values, derivative and the Arrhenius Plot for the BAP1 strand is presented in Figure 2. The figures were drawn using the basic plotting function in R. The fitted values (Figure 2(a)) show pronounced hysteresis which is reflected in the difference in the values of $T_{1/2\text{-melt}}$ and $T_{1/2\text{-anneal}}$ as observed in Figure 2(b). The Arrhenius plot is in Figure 2(c).

In Table 1 we present the values of the kinetic and thermodynamic parameters of the G-quadruplex formation of BAP1 and CCDC64 obtained using our method. The quoted values of k_{on} and k_{off} are for 25.0°C. These values were found by extrapolating the linear fits of their corresponding values near $T_{1/2\text{-anneal}}$ and $T_{1/2\text{-melt}}$ in the Arrhenius Plot (see equations (22) and (23)). The values of T_m turns out to be 71.0°C and 67.7°C respectively. These values are pretty close to corresponding temperatures reported by Pandey et al. (2013), which are 73.0°C and 70.0°C for BAP1 and CCDC64 respectively. This shows that using the proposed procedure one can compute the value of T_m quite accurately from non-equilibrium thermal curves.

6.0.2. *LNA modified duplex formation.* For our second illustrative example, we consider data from a hybridization experiment of duplex formation consisting of PuP (5' - AGAAAGAGAAGA - 3') and Py0 (5' - TCTTTCTCTTCT - 3'). These sequences were used by Bhattacharyya et al. (2011), who further introduced LNA modification at the cytosine bases of Py0.

They performed the melting and annealing both with a temperature gradient of 0.5°C per minute with $C = 10^{-6}$ mol and reported marked hysteresis in the hybridization of PuP and LNA modified Py0. Extent

TABLE 1. Kinetic and thermodynamic parameters of the hybridization experiment of intramolecular RNA G-Quadruplexes formation from Pandey et al. (2013). The quoted values of k_{on} , k_{off} , $T\Delta S^\circ$ and ΔG_T° are those predicted at 25.0° C by the linear fits of the Arrhenius plot.

| Strand | $T_{1/2\text{-anneal}}$ | $T_{1/2\text{-melt}}$ | k_{on} ($M^{-1}s^{-1}$) | k_{off} (s^{-1}) | ΔH° (kcal mol^{-1}) | $T\Delta S^\circ$ (kcal mol^{-1}) | ΔG_T° (kcal mol^{-1}) |
|--------|-------------------------|-----------------------|---------------------------------------|----------------------------------|--|---|--|
| BAP1 | 71.0°C | 75.0°C | 2.67 | 1.75×10^{-4} | -43.0 | -37.2 | -5.74 |
| CCDC64 | 66.6°C | 70.8°C | 23.6 | 1.32×10^{-4} | -57.5 | -50.3 | -7.21 |

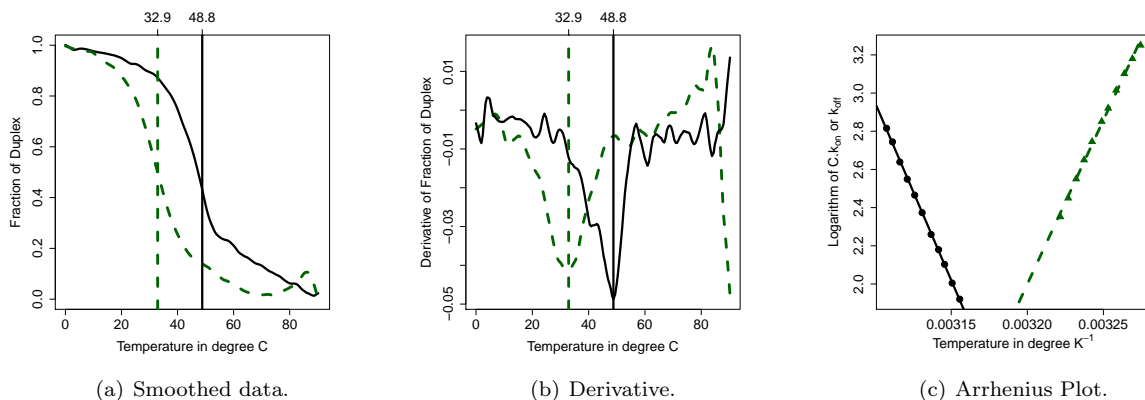


FIGURE 3. Smoothed curve 3(a), Derivative 3(b) and Arrhenius Plot 3(c) for PuP/Py4 sequence as described in Bhattacharyya et al. (2011). The solid lines correspond to melting and the dashed lines correspond to annealing. The fraction of the duplex was calculated using Equation (7). The results were obtained from the proposed software. Note that our value for $T_{1/2}$ -melt and $T_{1/2}$ -anneal are close to the values of these parameters reported in Bhattacharyya et al. (2011).

of this hysteresis increased with the number of LNA modifications. We choose data from the hybridization of Py0 and Py4 ($5' - \text{TC}^{\text{L}}\text{TTTC}^{\text{L}}\text{TC}^{\text{L}}\text{TTC}^{\text{L}}\text{T} - 3'$), with LNA modification (denoted by C^{L}) on all four cytosine bases of Py0 for our purpose.

The hybridization of PuP/Py4 shows a marked Hysteresis for both pH (5.0 and 7.0) values. We present the fitted values, derivative and the Arrhenius Plot for pH 7.0 in Figure 3. In Table 2 the values of the kinetic and thermodynamic parameters of the hybridization experiment of PuP/Py0 and PuP/Py4 obtained using our method are presented. As before the quoted values of k_{on} and k_{off} are for 25.0° C and were obtained by extrapolating the linear fits in the Arrhenius Plot as described above.

7. CONCLUSION

In this article we describe a statistical procedure to analyze UV thermal curves from nucleic acid hybridization experiments showing hysteresis. Our procedure provides an unified tool to obtain all the kinetic and thermodynamic parameters of the experiment. We use a statistical technique called *local Polynomial regression* to smooth the experimental data and to find the derivative of the smoothed curve. The kinetic rate constants are then computed by solving a pair of linear equations. The thermodynamic constants are obtained from these kinetic constants *via* the Arrhenius plot. All the tools used in our package are available

TABLE 2. Kinetic and thermodynamic parameters of the hybridization experiment of PuP/Py0 and PuP/Py4 reported in Bhattacharyya et al. (2011). The quoted values of k_{on} , k_{off} , ΔH° , $T\Delta S^\circ$ and ΔG_T° are those predicted at 25.0°C by the linear fits of the Arrhenius plot.

| Strand | pH | $T_{1/2}$ -anneal | $T_{1/2}$ -melt | k_{on} ($M^{-1}s^{-1}$) | k_{off} (s^{-1}) | ΔH° (kcal mol^{-1}) | $T\Delta S^\circ$ (kcal mol^{-1}) | ΔG_T° (kcal mol^{-1}) |
|--------|-----|-------------------|-----------------|---------------------------------------|----------------------------------|--|---|--|
| Py0 | 5.0 | 25.5°C | 28.5°C | 5.07×10^7 | 11.8 | -59.4 | -50.3 | -9.11 |
| | 7.0 | 15.4°C | 19.2°C | 1.67×10^7 | 16.9 | -40.8 | -32.6 | -8.23 |
| Py4 | 5.0 | 53.0°C | 71.0°C | 1.44×10^{10} | 4.70×10^{-6} | -116.0 | -94.4 | -21.2 |
| | 7.0 | 32.9°C | 48.8°C | 8.50×10^7 | 0.18 | -66.1 | -54.2 | -11.9 |

for free from a statistical software called R. An user-friendly web based version of our package is under construction and will be made available soon.

ACKNOWLEDGEMENT

J. Bhattacharyya was a recipient of the Research Associateship from the CSIR (Govt. of India). D. Miyoshi is supported in part by Grants-in-Aid for Scientific Research, the “Core Research” project (2009 – 2014) from the Ministry of Education, Culture, Sports, Science and Technology, Japan, the Hirao Taro Foundation of the Konan University Association for Academic Research, and the Long-Range Research Initiative Project of Japan Chemical Industry Association. S. Chaudhuri is partially supported by the Grant R-155-000-111-112 from National University of Singapore. Support and cooperation from the members of the Biophysical Chemistry Laboratory, Indian Institute of Chemical Biology and Departments of Chemistry and Computer Science, National Institute of Technology Nagaland are gratefully acknowledged.

REFERENCES

- Nakano, S.; Karimata, H.; Ohmichi, T.; Kawakami, J.; Sugimoto, N. *Journal of the American Chemical Society* **2004**, *126*, 14330–14331.
- Miyoshi, D.; Karimata, H.; Sugimoto, N. *Journal of the American Chemical Society* **2006**, *128*, 7957–7963.
- Miyoshi, D.; Nakamura, K.; Tateishi-Karimata, H.; Ohmichi, T.; Sugimoto, N. *Journal of the American Chemical Society* **2009**, *131*, 3522–3531.
- Ray, A.; Maiti, M.; Nandy, A. *Comput. Biol. Med.* **1996**, *26*, 497–503.
- Mirzoev, A.; Lyubartsev, A. P. *Journal of Chemical Theory and Computation* **2013**, *9*, 1512–1520.
- Mergny, J.-L.; Lacroix, L. *Oligonucleotides* **2003**, 515–537.
- Sugimoto, N.; Wu, P.; Hara, H.; Kawamoto, Y. *Biochemistry* **2001**, 9396–9405.
- Rougée, M.; Faucon, B.; Mergny, J. L.; Bercelo, F.; Giovannangeli, C.; Garestier, T.; Hélène, C. *Biochemistry* **1992**, 9269–9278.
- Cantor, C. R.; Schimmel, P. R. *Biophysical Chemistry Part III*; W. H. Freeman and Company, 1980.
- Brown, N. M.; Rachwal, P. A.; Brown, T.; Fox, K. R. *Org. Biomol. Chem.* **2005**, *3*, 4153–4157.
- Anshelevich, V. V.; Vologodskii, A. V.; Lukashin, A. V.; Frank-Kamenetskii, M. D. *Biopolymers* **1984**, *23*, 39–58.
- Hickman, D. T.; King, P. M.; Cooper, M. A.; Slater, J. M.; Micklefield, J. *Chem. Commun.* **2000**,
- Kaur, H.; Babu, B. R.; Maiti, S. *Chem. Rev.* **2007**, *107*, 4672–4692.
- Bhattacharyya, J.; Maiti, S.; Muhuri, S.; Nakano, S.; Miyoshi, D.; Sugimoto, N. *Biochemistry* **2011**, 7414–7425.
- Blaskó, A.; Dempcy, R. O.; Minyat, E. E.; Bruice, T. C. *Journal of the American Chemical Society* **1996**, *118*, 7892–7899.
- Arya, D. P.; Bruice, T. C. *Proceedings of the National Academy of Sciences* **1999**, *96*, 4384–4389.
- Kumar, N.; Nielsen, K. E.; Maiti, S.; Petersen, M. *J. Am. Chem. Soc.* **2006**, *128*, 14–15.
- Lesnik, E. A.; Risen, L. M.; Driver, D. A.; Griffith, M. C.; Sprankle, K.; Freier, S. M. *Nucleic Acids Research* **1997**, *25*, 568–574.
- Mergny, J.-L.; De Cian, A.; Ghelab, A.; Saccà, B.; Lacroix, L. *Nucleic Acids Research* **2005**, *33*, 81–94.
- Tran, P.; De Cian, A.; Gros, J.; Moriyama, R.; Mergny, J.-L. In *Quadruplex Nucleic Acids*; Chaires, J. B., Graves, D., Eds.; Topics in Current Chemistry; Springer Berlin Heidelberg, 2013; Vol. 330; pp 243–273.
- Mergny, J.-L.; Lacroix, L. *Current Protocols in Nucleic Acid Chemistry*; John Wiley & Sons, Inc., 2001.
- Saccà, B.; Lacroix, L.; Mergny, J.-L. *Nucleic Acids Research* **2005**, *33*, 1182–1192.
- Zhang, A. Y. Q.; Balasubramanian, S. *Journal of the American Chemical Society* **2012**, *134*, 19297–19308.
- Pandey, S.; Agarwal, P.; Maiti, S. *J. Phys. Chem. B* **2013**, 6896–6905.
- Kaur, H.; Wengel, J.; Maiti, S. *Biochemistry* **2008**, *47*, 1218–1227.
- Das, A.; Bhadra, K.; Suresh Kumar, G. *PLOS One* **2011**, *6*, e23186.
- Bhadra, K.; Suresh Kumar, G. *Med. Res. Rev.* **2011**, *31*, 821–862.
- Saha, I.; Hossain, M.; Suresh Kumar, G. *J. Phys. Chem. B.* **2010**, *114*, 15278–15287.
- R Core Team, R: A Language and Environment for Statistical Computing. R Foundation for Statistical Computing: Vienna, Austria, 2012; ISBN 3-900051-07-0.

Arora, A.; Maiti, S. *J. Phys. Chem. B* **2009**, *113*, 10515–10520.
Mergny, J.-L.; Lacroix, L. *Current protocols in Nucleic acid Chemistry* **2009**,
Savitzky, A.; Golay, M. J. E. *Anal. Chem.* **1964**, *36*, 1627–1639.
Marchand, P.; Marmet, L. *Rev. Sci. Instrum.* **1983**, *54*, 1034–1041.
Brabanter, K. D.; Brabanter, J. D.; Moor, B. D.; Gijbels, I. *J. Mach. Learn. Res.* **2013**, *14*, 281–301.
Wand, M. P.; Jones, M. C. *Kernel Smoothing*; Chapman & Hall/CRC: Boca Raton, FL, 1995.
Herrmann, E.; Maechler, M. *lokern: Kernel Regression Smoothing with Local or Global Plug-in Bandwidth*.
2013.
Email address: jhimli.bhattacharyya@gmail.com

DEPARTMENT OF CHEMISTRY, NATIONAL INSTITUTE OF TECHNOLOGY NAGALAND, CHUMUKEDIMA, DIMAPUR, NAGALAND, 797
103, INDIA.

BIOPHYSICAL CHEMISTRY LABORATORY, CSIR-INDIAN INSTITUTE OF CHEMICAL BIOLOGY, 4 RAJA S. C. MULLICK ROAD,
JADAVPUR, KOLKATA 700 032, INDIA

PROTEOMICS AND STRUCTURAL BIOLOGY UNIT, INSTITUTE OF GENOMICS AND INTEGRATIVE BIOLOGY, CSIR, MALL ROAD,
DELHI, 110 007, INDIA

FRONTIERS OF INNOVATIVE RESEARCH IN SCIENCE AND TECHNOLOGY (FIRST), KONAN UNIVERSITY, 7-1-20 MINATOJIMA-
MINAMIMACHI, CHUO-KU, KOBÉ 650-0047, JAPAN

Email address: stasc@nus.edu.sg

DEPARTMENT OF STATISTICS AND APPLIED PROBABILITY, NATIONAL UNIVERSITY OF SINGAPORE, 6 SCIENCE DRIVE 2, SINGA-
PORE 117 546